Biochemical Pharmacology 83 (2012) 1229–1240

Contents lists available at SciVerse ScienceDirect

Biochemical Pharmacology

journal homepage: www.elsevier.com/locate/biochempharm

Thiostrepton is an inducer of oxidative and proteotoxic stress that impairs viability of human melanoma cells but not primary melanocytes

Shuxi Qiao, Sarah D. Lamore, Christopher M. Cabello, Jessica L. Lesson, José L. Muñoz-Rodriguez, Georg T. Wondrak *

Department of Pharmacology and Toxicology, College of Pharmacy & Arizona Cancer Center, University of Arizona, 1515 North Campbell Avenue, Tucson, AZ 85724, USA

ARTICLE INFO

Article history:
Received 29 November 2011
Accepted 24 January 2012
Available online 1 February 2012

Keywords:
Malignant melanoma
Oxidative and proteotoxic stress
Heat shock response
Proteasome
Thiostrepton

ABSTRACT

Pharmacological induction of oxidative and proteotoxic stress has recently emerged as a promising strategy for chemotherapeutic intervention targeting cancer cells. Guided by a differential phenotypic drug screen for novel lead compounds that selectively induce melanoma cell apoptosis without compromising viability of primary human melanocytes, we have focused on the cyclic pyridinyl-polythiazolyl peptide-antimicrobial thiostrepton. Using comparative gene expression-array analysis, the early cellular stress response induced by thiostrepton was examined in human A375 metastatic melanoma cells and primary melanocytes. Thiostrepton displayed selective antimelanoma activity causing early induction of proteotoxic stress with massive upregulation of heat shock (*HSPA6*, *HSPA1A*, *DNAJB4*, *HSPB1*, *HSPH1*, *HSPA1L*, *CRYAB*, *HSPA5*, *DNAJA1*), oxidative stress (*HMOX1, GSR, SOD1*), and ER stress response (*DDIT3*) gene expression, confirmed by immunodetection (Hsp70, Hsp70B′, HO-1, phospho-eIF2α). Moreover, upregulation of p53, proapoptotic modulation of Bcl-2 family members (Bax, Noxa, Mcl-1, Bcl-2), and induction of apoptotic cell death were observed. Thiostrepton rapidly induced cellular oxidative stress followed by inactivation of chymotrypsin-like proteasomal activity and melanoma cell-directed accumulation of ubiquitinated proteins, not observed in melanocytes that were resistant to thiostrepton-induced apoptosis. Proteotoxic and apoptogenic effects were fully antagonized by antioxidant intervention. In RPMI 8226 multiple myeloma cells, known to be exquisitely sensitive to proteasome inhibition, early proteotoxic and apoptogenic effects of thiostrepton were confirmed by array analysis indicating pronounced upregulation of heat shock response gene expression. Our findings demonstrate that thiostrepton displays dual activity as a selective prooxidant and proteotoxic chemotherapeutic, suggesting feasibility of experimental intervention targeting metastatic melanoma and other malignancies including multiple myeloma.

1. Introduction

Melanoma is a malignant melanocyte-derived tumor causing the majority of deaths attributed to skin cancer [1]. Despite recent progress in the design of targeted therapies such as the V600E-mutation directed BRAF-inhibitor vemurafenib, efficacy of chemotherapeutic intervention directed against the metastatic stage of the disease remains limited, and an urgent need exists for the identification and development of improved molecular agents targeting metastatic melanoma cells [2].

The causative involvement of altered redox homeostasis and reactive oxygen species (ROS)-dependent signaling in the control of survival, proliferation, and invasiveness of melanoma and other cancer cells has recently been substantiated [3–6]. Feasibility of redox-directed intervention for the targeted chemotherapeutic induction of cancer cell apoptosis has been explored earlier based on the rational that small molecule prooxidant intervention may cause cytotoxic deviations from redox homeostasis that induce apoptosis in malignant cells, already exposed to high constitutive levels of ROS, without compromising viability of non-transformed cells [6–9]. Indeed, numerous preclinical and clinical studies have explored the tumor-directed efficacy of experimental and investigational redox chemotherapeutics including piperlongumine [10],

Abbreviations: AV, annexinV; BSO, L-buthionine-S,R-sulfoximine; DCFH-DA, 2′,7′-dichlorodihydrofluorescein diacetate; DDIT3, DNA-damage-inducible transcript 3; EGR1, early growth response gene 1; FITC, fluorescein isothiocyanate; GSH, glutathione; HEMa, primary human epidermal melanocyte; Hsp, heat shock protein; HSPA1A, heat shock 70 kDa protein 1A; HSPA6, heat shock 70 kDa protein 6; HMOX1, heme oxygenase-1; NAC, N-acetyl-L-cysteine; PI, propidium iodide; ROS, reactive oxygen species; SDS-PAGE, sodium dodecylsulfate polyacrylamide gel electrophoresis; T, thiostrepton; Ub, ubiquitin.

* Corresponding author at: University of Arizona, Arizona Cancer Center, 1515 North Campbell Avenue, Tucson, AZ 85724, USA. Tel.: +1 520 626 9017; fax: +1 520 626 3797.
E-mail address: wondrak@pharmacy.arizona.edu (G.T. Wondrak).

0006-2952/$ – see front matter © 2012 Elsevier Inc. All rights reserved.
doi:10.1016/j.bcp.2012.01.027

β-phenylethyl isothiocyanate [11], mangafodipir [12], DCPIP (2,6-dichlorophenolindophenol) [13], NOV-002 [14], NSC 689534 [15], and PX-12 [16], as reviewed recently [6,9,17–19].

Using a differential phenotypic drug screen for novel redox-directed leads that selectively induce melanoma cell apoptosis without compromising viability of primary human melanocytes, we have recently identified the antimalarial dihydroartemisinin (DHA) as a prooxidant experimental chemotherapeutic that induces iron-dependent Noxa-mediated apoptosis in melanoma cells [20]. As part of our screening campaign we also focussed on the natural product thiostrepton, a compound selected for further activity screening based on its known ability to induce cellular oxidative stress [21]. Thiostrepton is a streptomycete-derived cyclic pyridinyl-polythiazolyl oligopeptide displaying potent antimicrobial activity based on targeting the bacterial 23S rRNA complexed with ribosomal protein L11 [22,23]. In addition, antimalarial activity of thiostrepton has been attributed to inhibition of the parasite proteasome [24]. Importantly, recent research has documented anticancer activity of this oligopeptide antibiotic assessed in murine MDA-MB-231 breast carcinoma and HepG2 hepatoma xenograft models [25]. Involvement of various mechanistic factors in cancer cell-directed cytotoxicity of thiostrepton has been demonstrated including inhibition of the Forkhead Box M1 (FoxM1) transcription factor [26,27], inhibition of proteasomal enzymatic activity [26,28,29], and mitochondrial alterations with prooxidant modulation of cellular redox homeostasis [21]. Pronounced induction of apoptotic cell death by thiostrepton has been documented earlier in cultured melanoma cell lines [30], and upregulation of oxidative stress in metastatic melanoma cells exposed to the combined action of arsenic trioxide and thiostrepton was observed upon prolonged exposure [21], but early molecular pathways underlying melanoma cell-directed cytotoxicity induced by thiostrepton remain largely undefined.

Using comparative gene expression array analysis as a discovery tool, we have monitored the thiostrepton-induced early cellular stress response that occurs at the transcriptional and protein level within hours of exposure in cultured metastatic melanoma cells and primary melanocytes. We report for the first time that thiostrepton displays activity as a selective antimelanoma agent that spares cultured primary melanocytes, causing early induction of oxidative and proteotoxic stress with massive upregulation of heat shock response gene expression and proapoptotic modulation of Bcl-2 family members in metastatic melanoma cells. Thiostrepton treatment was associated with rapid inactivation of proteasome-dependent proteolytic activity and melanoma cell-directed accumulation of ubiquitinated proteins that was not detected in melanocytes. These early proteotoxic and apoptogenic effects were also observed in thiostrepton-treated myeloma cells known to be exquisitely sensitive to chemotherapeutic proteasome inhibition.

2. Materials and methods

2.1. Chemicals

The cell-permeable pancaspase inhibitor zVADfmk, the cell permeable caspase 8 inhibitor Ac-AAVALLPAVLLALLAP-IETD-CHO, and thiostrepton (≥98% purity) were from EMD Biosciences-Calbiochem (San Diego, CA, USA). All other chemicals were purchased from Sigma Chemical Co (St. Louis, MO, USA).

2.2. Cell culture

A375 and G-361 human melanoma cells from ATCC (Manassas, VA, USA) were cultured in RPMI medium containing 10% FBS and 2 mM L-glutamine or McCoy's 5a medium containing 10% FBS, respectively. RPMI 8226 human myeloma cells (ATCC) were maintained in RPMI medium (10% FBS). Primary human epidermal melanocytes (adult skin, lightly pigmented: HEMa-LP from Cascade Biologics, abbreviated HEMa) were cultured using Medium 154 medium supplemented with HMGS-2 growth supplement. HEMa cells were passaged using recombinant trypsin/EDTA and defined trypsin inhibitor. Cells were maintained at 37 °C in 5% CO_2, 95% air in a humidified incubator.

2.3. Human stress and toxicity pathfinder^{TM} RT^2 profiler^{TM} PCR expression array

After pharmacological exposure, total cellular RNA (3×10^6 A375 cells) was prepared according to a standard procedure using the RNeasy kit (Qiagen, Valencia, CA, USA). Reverse transcription was performed using the RT^2 First Strand kit (SuperArray, Frederick, MD, USA) and 5 μg total RNA as described previously [13,20]. The RT^2 Human Stress and Toxicity Pathfinder^{TM} PCR Expression Array (SuperArray) profiling the expression of 84 stress-related genes was run using the following PCR conditions: 95 °C for 10 min, followed by 40 cycles of 95 °C for 15 sec alternating with 60 °C for 1 min (Applied Biosystems 7000 SDS). Gene-specific product was normalized to GAPDH and quantified using the comparative ($\Delta\Delta C_t$) C_t method as described in the ABI Prism 7000 sequence detection system user guide as published earlier [13,31,32]. Expression values were averaged across three independent array experiments, and standard deviation was calculated for graphing.

2.4. HSPA1A, HSPA6, and HMOX1 expression analysis by real time RT-PCR

For expression analysis by real time RT-PCR, total cellular RNA (3×10^6 cells) was prepared using the RNEasy kit from Qiagen (Valencia, CA, USA). Reverse transcription was performed using TaqMan Reverse Transcription Reagents (Roche Molecular Systems, Branchburg, NJ, USA) and 200 ng of total RNA in a 50 μl reaction. Reverse transcription was primed with random hexamers and incubated at 25 °C for 10 min followed by 48 °C for 30 min, 95 °C for 5 min, and a chill at 4 °C. Each PCR reaction consisted of 3.75 μl of cDNA added to 12.5 μl of TaqMan Universal PCR Master Mix (Roche Molecular Systems), 1.25 μl of gene-specific primer/probe mix (Assays-by-Design; Applied Biosystems, Foster City, CA) and 7.5 μl of PCR water. PCR conditions were: 95 °C for 10 min, followed by 40 cycles of 95 °C for 15 s, alternating with 60 °C for 1 min using an Applied Biosystems 7000 SDS and Applied Biosystems' Assays On Demand primers specific to *HSPA6* (assay ID Hs00275682_s1), *HSPA1A* (assay ID Hs00359163_s1), *HMOX1* (assay ID Hs00157965_m1), and *GAPDH* (assay ID Hs99999905_m1). Gene-specific product was normalized to *GAPDH* and quantified using the comparative ($\Delta\Delta C_t$) C_t method as described before [13,31,32].

2.5. Immunoblot analysis

Sample preparation, SDS-PAGE, transfer to nitrocellulose, and development occurred as described earlier [13,31,33]. Gel percentage was 12%. Antibodies were purchased from the following manufacturers: Cell Signaling Technology (Danvers, MA): anti-phospho-eIF2α, anti-eIF2α (total), anti-Bcl-2 rabbit monoclonal; anti-Bax, anti-Mcl-1 rabbit polyclonal. Santa Cruz Biotechnology (Santa Cruz, CA): anti-p53 mouse monoclonal; EMD Chemicals (Gibbstown, NJ): mouse anti-Noxa IgG (OP180; 1:1000). Enzo Life Sciences (Farmingdale, NY): anti-Hsp70. anti-Hsp60, anti-Hsp90 mouse monoclonal. The following secondary antibodies were used: HRP-conjugated goat anti-rabbit antibody or HRP-conjugated goat anti-mouse antibody (Jackson Immunological Research, West Grove, PA). Equal protein loading was examined by β-actin-detection using a mouse anti-actin monoclonal antibody (Sigma).

2.6. Hsp70B′ ELISA

The enzyme-linked immunosorbent assay for heat shock 70 kDa protein 6 (also called Hsp70B′) was performed in 96 well format on cell lysates extracted from treated cells following kit instructions ('Hsp70B prime' ELISA Kit; Assay Designs, Ann Arbor, MI) as published recently [13]. Briefly, 1×10^6 cells were seeded per T-75 flask one day before treatment. Cells (3×10^6 per group) were exposed to test compound for 6 h (37 °C, 5% CO_2) and then harvested, washed with PBS, and lysed in 1× extraction reagent. After protein quantification using the BCA assay, samples were diluted to a range within the Hsp70B′ standard curve and processed according to the manufacturer's instructions. Absorbance (450 nm) was determined on a microtiter plate reader (Versamax, Molecular Devices, Sunnyvale, CA, USA). Data represent the average of three independent experiments.

2.7. Cell death analysis

Viability and induction of cell death (early and late apoptosis/necrosis) were examined by annexinV-FITC (AV)/propidium iodide (PI) dual staining of cells followed by flow cytometric analysis as published previously [34]. Cells (100,000) were seeded on 35 mm dishes and received drug treatment 24 h later. Cells were harvested at various time points after treatment and cell staining was performed using an apoptosis detection kit according to the manufacturer's specifications (APO-AF, Sigma).

2.8. Transmission electron microscopy

Cells were fixed in situ with 2.5% glutaraldehyde in 0.1 M cacodylate buffer (pH7.4), postfixed in 1% osmium tetroxide in cacodylate buffer, washed, scraped and pelleted. Cells were then stained in 2% aqueous uranyl acetate, dehydrated through a graded series (50, 70, 90, and 100%) of ethanol and infiltrated with Spurr's resin, then allowed to polymerize overnight at 60 °C. Sections (50 nm) were cut, mounted onto uncoated 150 mesh copper grids, and stained with 2% lead citrate. Sections were examined in a CM12 Transmission Electron Microscope (FEI, Hillsboro, OR) operated at 80 kV with digital image collection (AMT, Danvers, MA).

2.9. Flow cytometric detection of cleaved procaspase-3

Treatment-induced proteolytic caspase-3 activation was examined using antibodies directed against cleaved/activated caspase-3 (Asp 175) (Alexa Fluor 488 conjugate, Cell Signaling) followed by flow cytometric analysis as published recently [31,34].

2.10. Homogeneous luminescent caspase-9 activity assay

The Caspase-Glo™ 9 Assay kit (Promega, Madison, WI) was used according to manufacturer's specifications. Cells were seeded at 10,000 cells/well of a white-walled 96-well plate. After 24 h, cells were treated with test compound, and caspase-9 dependent cleavage of a luminogenic caspase-9 substrate (Z-LEHD-luciferin) was determined at specific time points after compound addition (0–12 h) using a Synergy 2 microplate reader (BioTek Instruments, Winooski, VT). Data are expressed as % activity relative to untreated control cells [means ± SD ($n = 3$)].

2.11. Proteasome activity assay

The Proteasome-Glo™ Cell-Based Assay kit (Promega) was used according to manufacturer's specifications. Cells were seeded at 4000 cells/well of an opaque 96-well plate. After 24 h, cells were treated with test compound. At the end of the treatment period, cells were washed with PBS and an equal volume of reagent containing the appropriate luminogenic substrate (Suc-LLVY-aminoluciferin or Z-LRR-aminoluciferin for chymotrypsin-like or trypsin-like proteasome activities, respectively) was added to each well (with inclusion of two proprietary inhibitors blocking non-specific proteases for determination of trypsin-like activity). Plates were incubated at room temperature (10 min) before measuring luminescence signal using a Synergy 2 microplate reader. Data are expressed as % activity relative to untreated control cells [means ± SD ($n = 3$)].

2.12. Detection of intracellular oxidative stress by flow cytometric analysis

Induction of intracellular oxidative stress by test compound was analyzed by flow cytometry using 2′,7′-dichlorodihydrofluorescein diacetate (DCFH-DA) as a sensitive non-fluorescent precursor dye according to a published standard procedure [34].

2.13. Determination of reduced cellular glutathione content

Intracellular reduced glutathione was measured using the GSH-Glo Glutathione assay kit (Promega; San Luis Obispo, CA) as described recently [35]. Cells were seeded at 100,000 cells/dish on 35 mm dishes. After 24 h, cells were treated with test compound. At selected time points after addition of test compound, cells were harvested by trypsinization and then counted using a Coulter counter. Cells were washed in PBS, and 10,000 cells/well (50 μl) were transferred onto a 96-well plate. GSH-Glo reagent (50 μl) containing luciferin-NT and glutathione-S-transferase was then added followed by 30 min incubation. After addition of luciferin detection reagent to each well (100 μl) and 15 min incubation luminescence reading was performed using a BioTek Synergy 2 Reader (BioTek, Winooski, VT, USA). Data are normalized to GSH content in untreated cells and expressed as means ± SD ($n = 3$).

2.14. Statistical analysis

Unless indicated differently, the results are presented as mean ± S.D. of at least three independent experiments, and data were analyzed employing *one-way* analysis of variance (*ANOVA*) with Tukey's post hoc test using the Prism 4.0 software. Differences were considered significant at $p < 0.05$. Means without a common letter differ ($p < 0.05$).

3. Results

3.1. Thiostrepton induces apoptosis in human A375 metastatic melanoma cells but not in primary epidermal melanocytes

First, differential apoptogenicity of thiostrepton was determined in A375 metastatic melanoma cells and primary human melanocytes (HEMa) using flow cytometric detection of annexinV-propidium iodide stained cells (Fig. 1A and B). Thiostrepton (1–10 μM, 24 h exposure) dose dependently induced cell death in A375 cells ($LD_{50} = 3.7 \pm 0.9$ μM; mean ± SD, $n = 3$), but did not affect viability of HEMa cells (10 and 20 μM, 24 h). Even at concentrations reaching the solubility limit of thiostrepton (>40 μM, 24 h) no reduction in HEMa cell viability was detected (data not shown). Further evidence supporting an apoptotic mode of thiostrepton-induced melanoma cell death was obtained by assessing thiostrepton cytotoxicity in the presence of the pancaspase inhibitor zVADfmk that completely blocked thiostrepton-induced cell death, an observation that was also made in human G361 metastatic melanoma cells

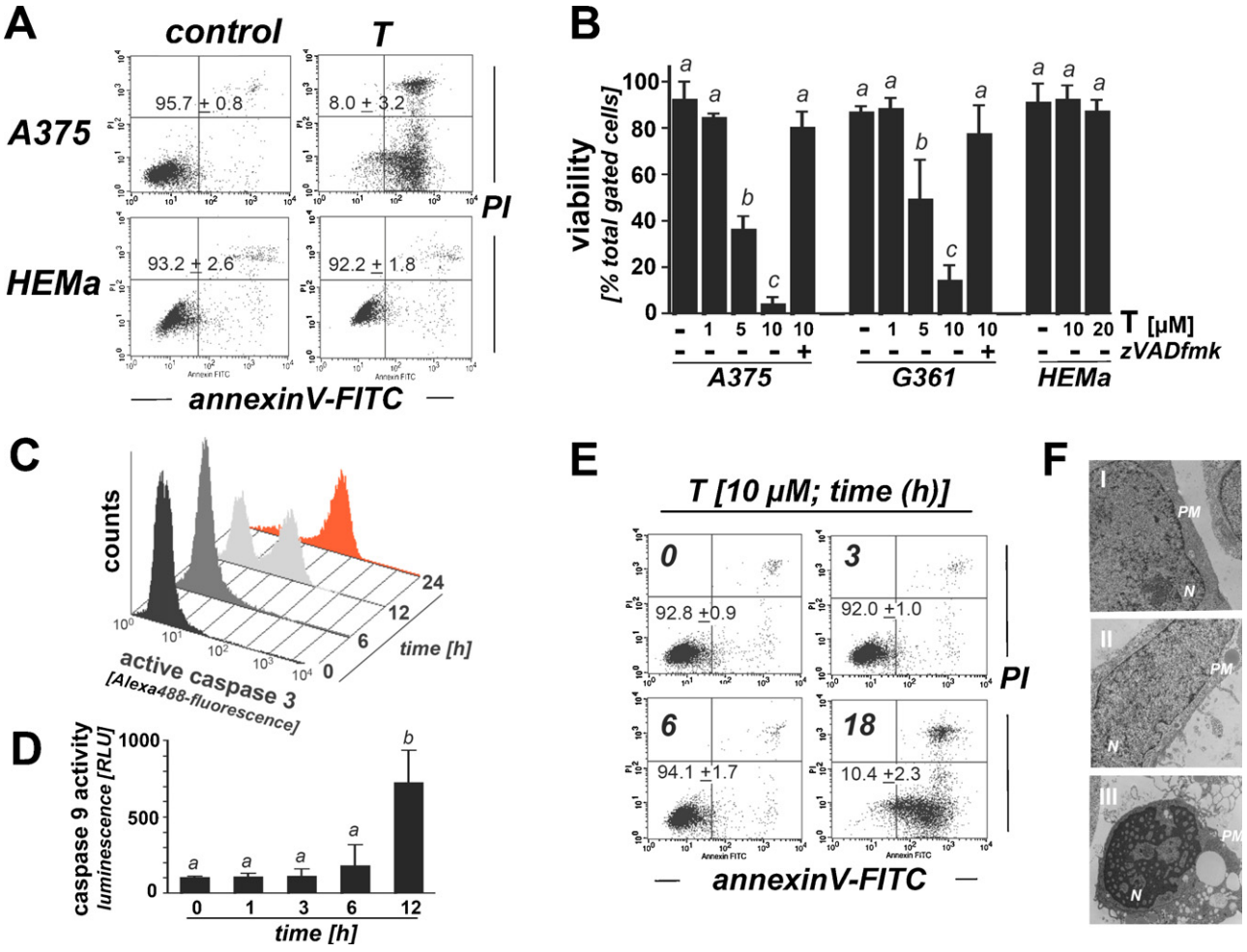

Fig. 1. Thiostrepton induces apoptotic death in human metastatic A375 and G361 melanoma cells but not in primary epidermal melanocytes. (A and B) Induction of A375 and human epidermal melanocyte (HEMa) cell death in response to thiostrepton exposure (T; 1, 5, 10 μM, 24 h) performed in the absence or presence of zVADfmk (40 μM) as assessed by flow cytometric analysis. The numbers (panel A) indicate viable (AV-, PI-) in percent of total gated cells (mean ± SD, $n = 3$). The bar graph (panel B) represents data obtained from three independent repeats involving metastatic melanoma cell lines (A375, G361) and primary melanocytes (HEMa). (C) T-induced (10 μM, 0–24 h) caspase-3 activation was examined in A375 cells by flow cytometric detection using an Alexa488-conjugated monoclonal antibody directed against proteolytically activated caspase 3. A representative experiment taken from three similar repeats is shown. (D) T-induced (10 μM, 0–12 h) caspase 9 activation was examined in A375 cells using a luminescent assay (based on conversion of a luminogenic caspase 9 substrate, Caspase-Glo™ 9 Assay; mean ± SD, $n = 3$). (E) Time course analysis (0–18 h continuous exposure, 10 μM T) of cell death performed in A375 cells. A representative experiment taken from three similar repeats is shown. (F) A375 cells [control (panel I) and T-treated (10 μM, 12 and 24 h; panels II and III, respectively)] were examined by transmission electron microscopy (direct magnification: ×8800; N, nucleus; PM, plasma membrane).

(Fig. 1B). Time course analysis of viability (Fig. 1E) and caspase-3 activation (Fig. 1C) revealed no significant changes after 6 h continuous exposure to thiostrepton, but proteolytic caspase-3 activation became evident upon 12 h continuous exposure [7.6 ± 3.3 fold upregulation based on Alexa-488 fluorescence intensity indicative of cleaved procaspase-3 (mean ± S.D.; $n = 3$)] and increased further within 24 h [41.7 ± 14.9 fold upregulation over control; (mean ± S.D.; $n = 3$)] (Fig. 1C). Massive induction of cell death became apparent at 18 h exposure time (Fig. 1E).

Further analysis revealed that cells were not protected from apoptosis when thiostrepton exposure occurred after pretreatment with Ac-AAVALLPAVLLALLAP-IETD-CHO, a peptide-based cell permeable caspase-8 inhibitor and molecular probe for the involvement of the extrinsic death receptor-mediated pathway of apoptosis (data not shown) [34]. In contrast, pronounced induction of caspase 9 proteolytic activity was detectable at early time points (12 h) in thiostrepton-exposed A375 cells employing a homogeneous luminescent assay (Fig. 1D). This finding is consistent with the causative involvement of the mitochondrial pathway of apoptotic cell death, where activation of caspase-9 occurs downstream of apoptosome formation, followed by caspase 9-dependent proteolytic activation of procaspase-3 and execution of cell death. Further morphological evidence in support of thiostrepton-induced apoptosis was obtained employing transmission electron microscopy that revealed early membrane blebbing (12 h exposure) followed by pronounced nuclear condensation (24 h exposure), both established hallmarks of cellular apoptosis (Fig. 1F, panels II and III).

3.2. Thiostrepton induces differential proteotoxic stress response gene expression in melanoma cells and melanocytes

To gain further mechanistic insight into the molecular events underlying melanoma cell-directed cytotoxicity of thiostrepton, modulation of stress and toxicity response gene expression was examined in A375 and HEMa cells exposed to thiostrepton using the RT^2 Human Stress and Toxicity Profiler™ PCR Expression Array technology (SuperArray, Frederick, MD) (Fig. 2A–C and G) [13,20,31]. To this end, early stress response gene expression changes were monitored after short term exposure (10 μM, 6 h

exposure), a time point at which melanoma cell viability was still maintained (Fig. 1C–E). Out of 84 stress-related genes contained on the array thiostrepton-induced expression changes in A375 cells affected 31 genes by at least two-fold over untreated control cells (Fig. 2A and C), whereas in melanocytes expression of only 13 genes was altered (Fig. 2B and C).

In A375 cells, massive upregulation of heat shock response gene expression by more than 10-fold was observed including genes encoding the heat shock proteins *Hsp70B′* (*HSPA6*; 5325-fold), *Hsp70 protein 1A* (*HSPA1A*; 92-fold), the Hsp70 cochaperone *DnaJ (Hsp40) homolog, subfamily B, member 4* (*DNAJB4*; 29 fold), *Hsp27 protein 1* (*HSPB1*; 21 fold), *Hsp105 protein 1* (HSPH1, 16-fold), *Hsp70*

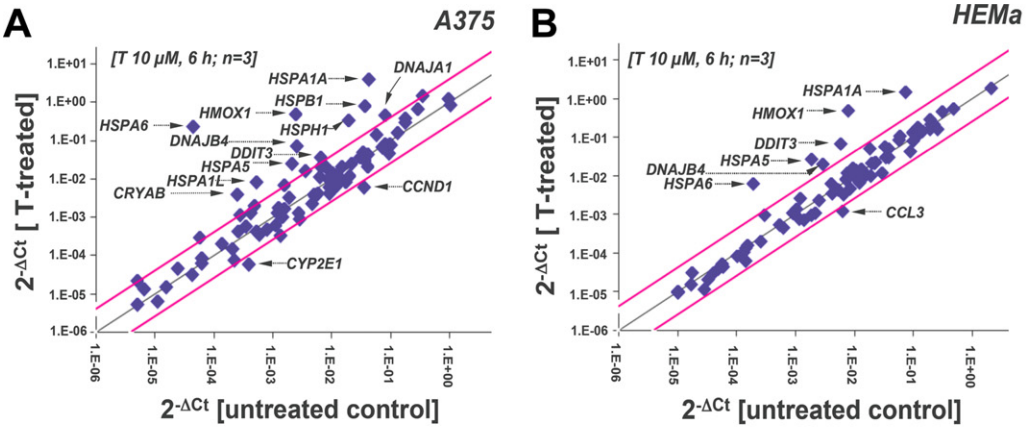

C

gene symbol (accession number)	gene name	A375 fold change (p<0.05)	HEMa fold change (p<0.05)
HSPA6 (NM_002155)	Heat shock 70 kDa protein 6 (HSP70BÕ)	5325.3	32.8
HMOX1 (NM_002133)	Heme oxygenase (decycling) 1	198.4	63.5
HSPA1A (NM_005345)	Heat shock 70 kDa protein 1A	92.4	19.7
DNAJB4 (NM_007034)	DnaJ (Hsp40) homolog, subfamily B, member 4	29.2	6.7
HSPB1 (NM_001540)	Heat shock 27 kDa protein 1	21.7	-
HSPH1 (NM_006644)	Heat shock 105 kDa/110 kDa protein 1	16.9	2.8
HSPA1L (NM_005527)	Heat shock 70 kDa protein 1-like	16.9	3.2
CRYAB (NM_001885)	Crystallin, alpha B	15.8	-
HSPA5 (NM_005347)	Heat shock 70 kDa protein 5	12.2	13.8
DNAJA1 (NM_001539)	DnaJ (Hsp40) homolog, subfamily A, member 1	6.0	-
DDIT3 (NM_004083)	DNA-damage-inducible transcript 3	5.4	11.4
GADD45A (NM_001924)	Growth arrest and DNA-damage-inducible. alpha	4.7	2.1
HSPA8 (NM_006597)	Heat shock 70 kDa protein 8	4.4	-
GDF15 (NM_004864)	Growth differentiation factor 15	4.3	-
HSPA2 (NM_021979)	Heat shock 70 kDa protein 2	4.1	4.2
PTGS1 (NM_000962)	Prostaglandin-endoperoxide synthase 1	4.0	-
HSP90AA2 (NG_005856)	Heat shock protein 90kDa alpha (cytosolic), class A member 2	3.2	-
GSR (NM_000637)	Glutathione reductase	3.1	-
HSPA4 (NM_002154)	Heat shock 70 kDa protein 4	2.7	-
SOD1 (NM_000454)	Superoxide dismutase 1, soluble	2.4	-
HSP90AB1 (NM_007355)	Heat shock protein 90kDa alpha (cytosolic), class B member 1	2.4	-
HSPD1 (NM_002156)	Heat shock 60kDa protein 1 (chaperonin)	2.2	-
BCL2L1 (NM_138578)	BCL2-like 1	-2.0	-
XRCC2 (NM_005431)	X-ray repair compl. defective repair in Chinese hamster cells 2	-2.0	-
NFKB1 (NM_00399	NF kappa light polypeptide gene enhancer in B-cells 1	-2.1	-
TP53 (NM_000546)	Tumor protein p53	-2.1	-
CYP1A1 (NM_000499)	Cytochrome P450, family 1, subfamily A, polypeptide 1	-2.9	-
IL1A (NM_000575)	Interleukin 1, alpha	-3.2	-
IL1B (NM_000576)	Interleukin 1, beta	-3.8	-
CCND1 (NM_053056)	Cyclin D1	-5.3	-
CYP2E1 (NM_000773)	Cytochrome P450, family 2, subfamily E, polypeptide 1	-6.1	-2.3
CCL4 (NM_053056)	Chemokine (C-C motif) ligand 4	-	-2.5
CCL3 (NM_000773)	Chemokine (C-C motif) ligand 3	-	-5.1

Fig. 2. Comparative gene expression array analysis of thiostrepton-treated human A375 metastatic melanoma and primary melanocytes. (A and B) The scatter blots depict differential gene expression as detected by the RT^2 Human Stress and Toxicity Profiler^{TM} PCR Expression Array technology [T: 10 µM, 6 h) in A375 melanoma cells (panel A) and melanocytes (panel B). Upper and lower lines: cut-off indicating fourfold up- or down-regulated expression, respectively. Arrays were performed in three independent repeats and analyzed using the two-sided Student's *t* test. (C) The table summarizes expression changes by at least twofold ($p < 0.05$). (D) T-modulation (10 µM, 1–6 h) of *HSPA1A* and *HSPA6* mRNA levels in A375 cells by independent real time RT-PCR analysis. (E) T-modulation (10 µM, 6 h) of Hsp70B′ prote*in* levels in A375 cells as assessed by ELISA and analyzed using the Student's *t* test. (F) T-modulation (10 µM, 1–6 h) of protein expression in A375 cells as assessed by immunoblot analysis. (G) Comparative analysis of heat shock- and ER stress-related gene expression changes at the mRNA level induced by T-treatment in A375 cells and melanocytes (as observed by expression array analysis performed in panels A and B); [$n = 3$, mean ± SD; ($p < 0.05$; T-treated versus untreated); * denotes statistically significant differences between HEMa and A375 cells ($^*p < 0.05$; $^{**}p < 0.01$; $^{***}p < 0.001$)]. (H) T-modulation (10 µM, 6 h) of protein expression in melanocytes as assessed by immunoblot analysis.

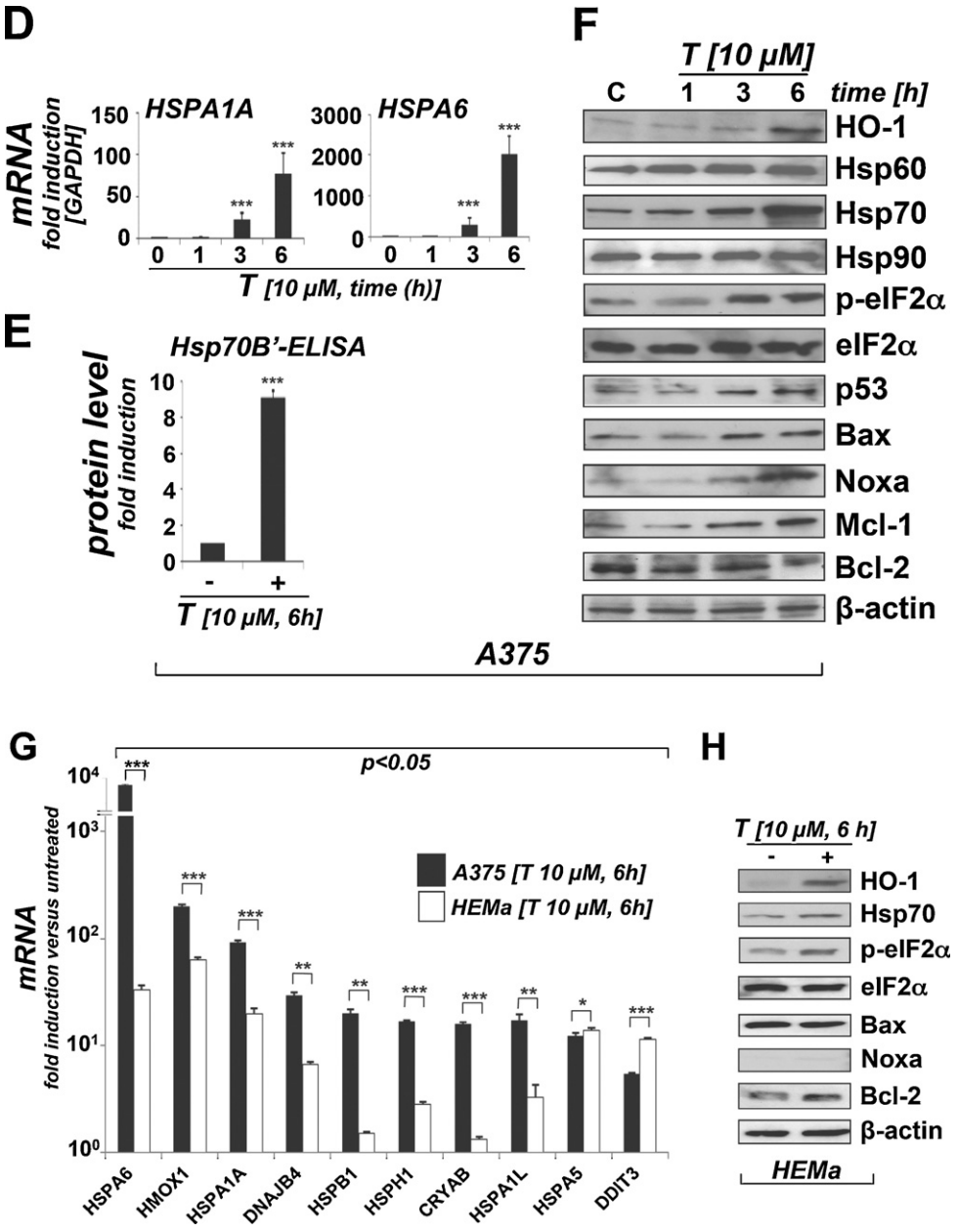

Fig. 2. (*Continued*).

protein 1-like (*HSPA1L*; 16-fold), *alpha-crystallin B chain* (*CRYAB*; 15-fold), and the endoplasmic reticulum-localized chaperone and proteotoxic stress sensor *Hsp70 protein 5* (*HSPA5*; 12-fold), also called *GRP-78* (*BiP*) [36]. Moreover, upregulation of genes encoding the heat shock protein and antioxidant enzyme *heme oxygenase-1* (*HMOX1*; 198-fold), the p53-regulated DNA damage inducible stress sensor *growth arrest and DNA-damage-inducible, alpha* (*GADD45A*; 4-fold), and the ER-stress responsive transcription factor *DNA damage inducible transcript 3/CHOP* (*DDIT3/GADD153*; 5-fold) was detected. Moreover, significant downregulation of *CCND1*, the gene encoding cyclin D1 (5-fold), was observed. Time course analysis using independent real time RT-PCR in A375 cells (1–6 h exposure, 10 μM thiostrepton) indicated that statistically significant upregulation of heat shock response gene expression (*HSPA6* and *HSPA1A*) occurred within 3 h exposure (Fig. 2D).

Consistent with gene expression array data obtained at the mRNA level at 6 h exposure time (Fig. 2A and C), massive induction of proteotoxic stress and heat shock response in A375 cells was also confirmed by immunoblot detection of HO-1 (heme oxygenase-1, encoded by *HMOX1*, a gene also responsive to oxidative stress) and Hsp70 (encoded by *HSPA1A*) observable within 3 h exposure (Fig. 2F). ELISA analysis confirmed upregulation of Hsp70B′, an Hsp70 family member encoded by *HSPA6*, known to be induced only under conditions of extreme cytotoxic stress and exquisitely sensitive to proteotoxic stress originating from proteasome inhibition (Fig. 2E) [33,37]. However, immunoblot analysis did not reveal significant quantitative changes affecting Hsp90 and Hsp60 expression (Fig. 2F), heat shock proteins that displayed only moderate upregulation at the transcriptional level in response to thiostrepton (*HSP90AA2* and *HSPD1*, respectively; Fig. 2A and C). Consistent with thiostrepton-induction of proteotoxic stress at early time points, the phosphorylated form (p-eIF2α) of eukaryotic Initiation Factor 2, subunit alpha (eIF2α), a key regulator of the cellular unfolded protein response (UPR) and sensitive indicator of proteotoxic ER stress, was detectable within 3 h exposure time (Fig. 2F) [36,38].

In addition, within 3–6 h exposure time, pro-apoptotic modulation affecting key regulators of mitochondrial apoptosis was observed at the protein level including the p53 downstream targets Bax, Noxa, Mcl-1, and Bcl-2 (Fig. 2F) [39,40]. Remarkably, p53 protein levels were increased within 3 h exposure time, and the p53 downstream targets Bax, a crucial mediator of mitochondrial membrane permeabilization, and Noxa, a BH3-domain only proapoptotic facilitator, were both upregulated at early time points (3 h continuous exposure; Fig. 2F). Intriguingly, protein levels of the antiapoptotic Bcl-2 family member Mcl-1, known to be targeted by Noxa towards proteasomal degradation, were first downregulated (1 h time point) but then underwent upregulation in response to thiostrepton exposure at later time points (3 and 6 h), a paradoxical effect that has been observed earlier in response to apoptogenic agents that interfere with proteasomal degradation of Mcl-1 [39–41]. In contrast, protein levels of the antiapoptotic modulator Bcl-2 were decreased within 6 h exposure.

Compared with effects observed in A375 metastatic melanoma cells, thiostrepton-induced expression changes observed in primary melanocytes were much less pronounced as judged by number of affected genes and magnitude of expression differential (Fig. 2B, C, G, H). Except for *HSPA5* mRNA levels, that were modulated equally in thiostrepton-exposed A375 melanoma cells and primary melanocytes, thiostrepton-induced upregulation of heat shock gene expression differed by up to more than two orders of magnitude (Fig. 2G). For example, *HSPA6*, upregulated in melanoma cells by more than 5000-fold, was induced only 33-fold in thiostrepton-exposed HEMa cells. Thiostrepton-induced changes observed in HEMa cells at the protein level were indicative of oxidative stress (HO-1), heat shock (Hsp70), and ER stress response (p-eIF2α), but no proapoptotic modulation of Noxa, Bax, or Bcl-2 was detected, consistent with the maintenance of HEMa cell viability in spite of thiostrepton exposure (Fig. 1A and B).

3.3. Thiostrepton-induced proteasome inhibition in metastatic melanoma cells and primary melanocytes

After detecting rapid induction of proteotoxic stress by thiostrepton and guided by earlier research that indicates thiostrepton-antagonism of proteasomal function, we directly tested inhibition of proteasomal enzymatic activity in cellular extracts and examined protein ubiquitination status (Fig. 3).

Using a luminescent protease assay that measures proteasome-dependent release of luciferin from specific precursor substrate peptides, we observed that thiostrepton acted as a partial inhibitor of proteasomal function, suppressing chymotrypsin-like activity by more than 50% of control levels within 6 h exposure in both A375 melanoma cells and primary melanocytes (Fig. 3B and D, respectively). A trend towards inhibitory activity targeting trypsin-like activity of the proteasome was observed but did not reach the level of statistical significance. Thiostrepton-induced proteasome inhibition reached the level of statistical significance within 3 h continuous exposure (Fig. 3B and D), an effect only observed in cells exposed to concentrations equal to or above 5 μM (data not shown and Fig. 4C).

Consistent with proteasomal inhibition, increased levels of ubiquitinated proteins were detected at early time points in A375 cells (Fig. 3A). In contrast, in melanocytes levels of ubiquitinated protein remained unaffected by thiostrepton treatment, and no increase was detected at any specific time point suggesting that these cells maintain clearance of ubiquitinated proteins even under conditions of partial proteasome inhibition (Fig. 3C and D).

As a positive control, the established proteasome inhibitor MG132 was used (10 μM, 6 h exposure time) (Fig. 3B and D, E) [39–41]. Indeed, chymotrypsin- and trypsin-like proteasome activity was strongly inhibited in both A375 cells and melanocytes (Fig. 3B and D, respectively), and pronounced accumulation of ubiquitinated

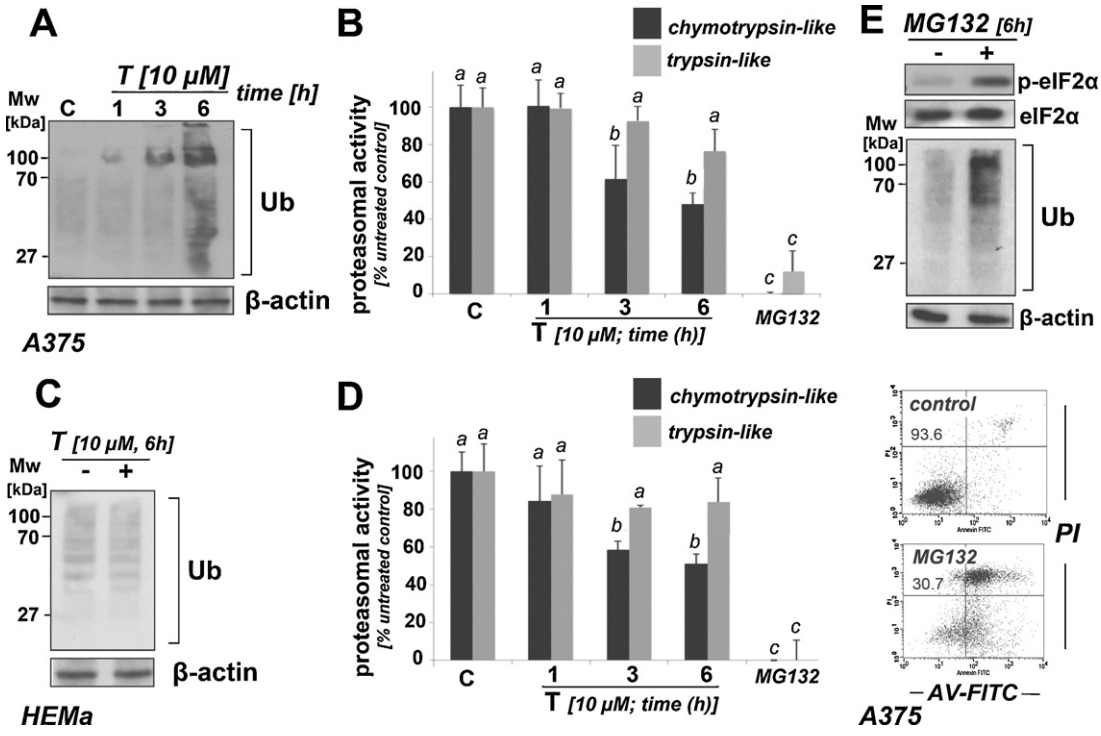

Fig. 3. Thiostrepton inhibits proteasome activity in A375 and HEMa cells, but causes accumulation of ubiquitinated proteins only in A375 cells. (A–D) A375 (panels A and B) and HEMa cells (panels C and D) were exposed to T (10 μM, up to 6 h). Cells were then harvested and processed for immunoblot analysis of protein ubiquitination (panels A and C) or luminescent analysis of proteasomal enzymatic activity (panels B and D). Treatment with MG132 (10 μM, 6 h; panels C and D) served as a positive control. Bar graphs represent data obtained from three independent repeats. (E) After MG132 exposure (10 μM) of A375 cells, immunoblot analysis of p-eIF2α and ubiquitination status was performed (6 h), and cell viability was determined (24 h exposure) by flow cytometric analysis. The numbers indicate viable (AV-, PI-) in percent of total gated cells. A representative experiment taken from three similar repeats is shown.

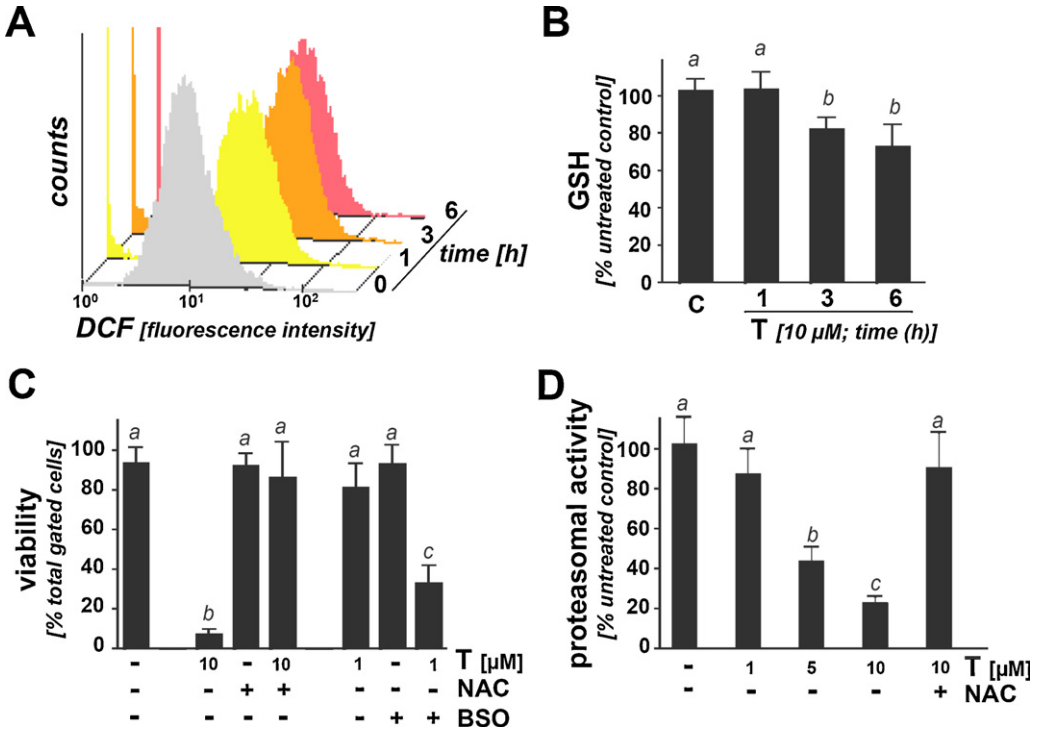

Fig. 4. Antioxidant treatment antagonizes thiostrepton-induced proteasome inhibition and cytotoxicity in A375 melanoma cells. (A) Induction of cellular oxidative stress as assessed by flow cytometric determination of 2′,7′-dichlorodihydrofluorescein diacetate (DCFH-DA) oxidation in response to T-exposure (10 μM, up to 6 h). Histograms depict one representative experiment out of three similar repeats. (B) Time course analysis of T-modulation of intracellular reduced glutathione content in A375 cells (10 μM, up to 6 h) normalized to cell number (mean ± SD, $n = 3$). (C) After preincubation (24 h) with BSO (1 mM) or NAC (10 mM), T-induced (1 and 10 μM, 24 h) A375 cell death was assessed by flow cytometric analysis of AV/PI-stained cells (mean ± SD, $n = 3$). (D) T-induced inhibition (1–10 μM, 6 h) of chymotrypsin-like proteasomal activity was examined with or without antioxidant treatment (NAC, 10 mM).

proteins was observed in thiostrepton-treated A375 cells (Fig. 3E). Interestingly, in these cells, eIF2α-phosphorylation, Hsp70 upregulation, and induction of apoptotic cell death occurred in the same manner as observed in response to thiostrepton (Fig. 3E), suggesting that proteasome inhibition may be a causative factor in thiostrepton-induced melanoma cell death, consistent with earlier reports on MG132- and bortezomib-induced cancer cell apoptosis [39,40].

3.4. Early induction of oxidative stress by thiostrepton: antioxidant intervention antagonizes proteasome inhibition and cytotoxicity

Next, upregulation of cellular oxidative stress in response to thiostrepton (10 μM, 1–6 h exposure time) was examined in A375 melanoma cells using flow cytometric determination of 2′,7′-dichlorodihydrofluorescein diacetate (DCFH-DA) oxidation (Fig. 4A). Mean intensity of cellular DCF-fluorescence increased by approximately five-fold within 1 h of thiostrepton-exposure (5.2 ± 0.9; mean ± SD; $n = 3$), a finding indicative of massive prooxidant deviations from cellular redox homeostasis at this early time point [34]. In contrast, thiostrepton-induced (10 μM, 1–6 h h exposure time) increase in DCF fluorescence in primary melanocytes was less pronounced, and a statistically significant increase by only 1.7 fold was observed at 6 h exposure time (1.7 ± 0.3; mean ± SD; $n = 3$; data not shown). Importantly, MG132 treatment of A375 cells (performed as indicated in Fig. 3E) was not associated with early induction of oxidative stress, and increased DCF fluorescence only became apparent at later time points (>6 h exposure time; data not shown), indicating that the molecular mechanism underlying induction of melanoma cell-directed oxidative stress may differ between thiostrepton and other proteasome inhibitors.

As an independent marker of oxidative stress, we then examined the occurrence of thiostrepton-induced glutathione depletion in melanoma cells and primary melanocytes. In A375 cells, significant reduction of reduced glutathione levels (approximately 30% of untreated control) was detectable within 3–6 h exposure (10 μM; Fig. 4B) before cell viability was impaired (Fig. 1D). In contrast, primary melanocytes were resistant to thiostrepton-induced glutathione depletion, and no statistically significant reduction was observed upon 6 h continuous exposure (data not shown).

Consistent with a causative role of oxidative stress and redox dysregulation in A375 cell death, significant sensitization to thiostrepton-induced cytotoxicity (10 μM, 24 h exposure) was observed in cells pre-exposed to L-buthionine-S,R-sulfoximine (BSO; 1 mM; 24 h preincubation; Fig. 4C), an established inhibitor of cellular glutathione biosynthesis [13]. Conversely, cell viability was largely maintained after preincubation with the glutathione precursor N-acetyl-L-cysteine (NAC, 10 mM) before exposure to thiostrepton (10 μM; 24 h; Fig. 4C). Strikingly, inhibition of proteasomal chymotrypsin-like activity (observed at thiostrepton concentrations ≥5 μM) was completely blocked by NAC pretreatment, suggesting that antioxidant intervention can antagonize thiostrepton-induced proteasome inactivation (Fig. 4D). However, the mechanism of NAC-dependent proteasome protection from thiostrepton-induced inactivation remains unresolved at this point. Indeed, other antioxidants including pegylated catalase, pegylated SOD, and L-ascorbate did not suppress thiostrepton-dependent cytotoxicity and proteasome inhibition (data not shown), and it is therefore possible that NAC protection against thiostrepton involves reductive and disulfide-directed (rather than free radical/-ROS-directed) reactivity associated with this nucleophilic thiol-reagent. Taken together, these data indicate that

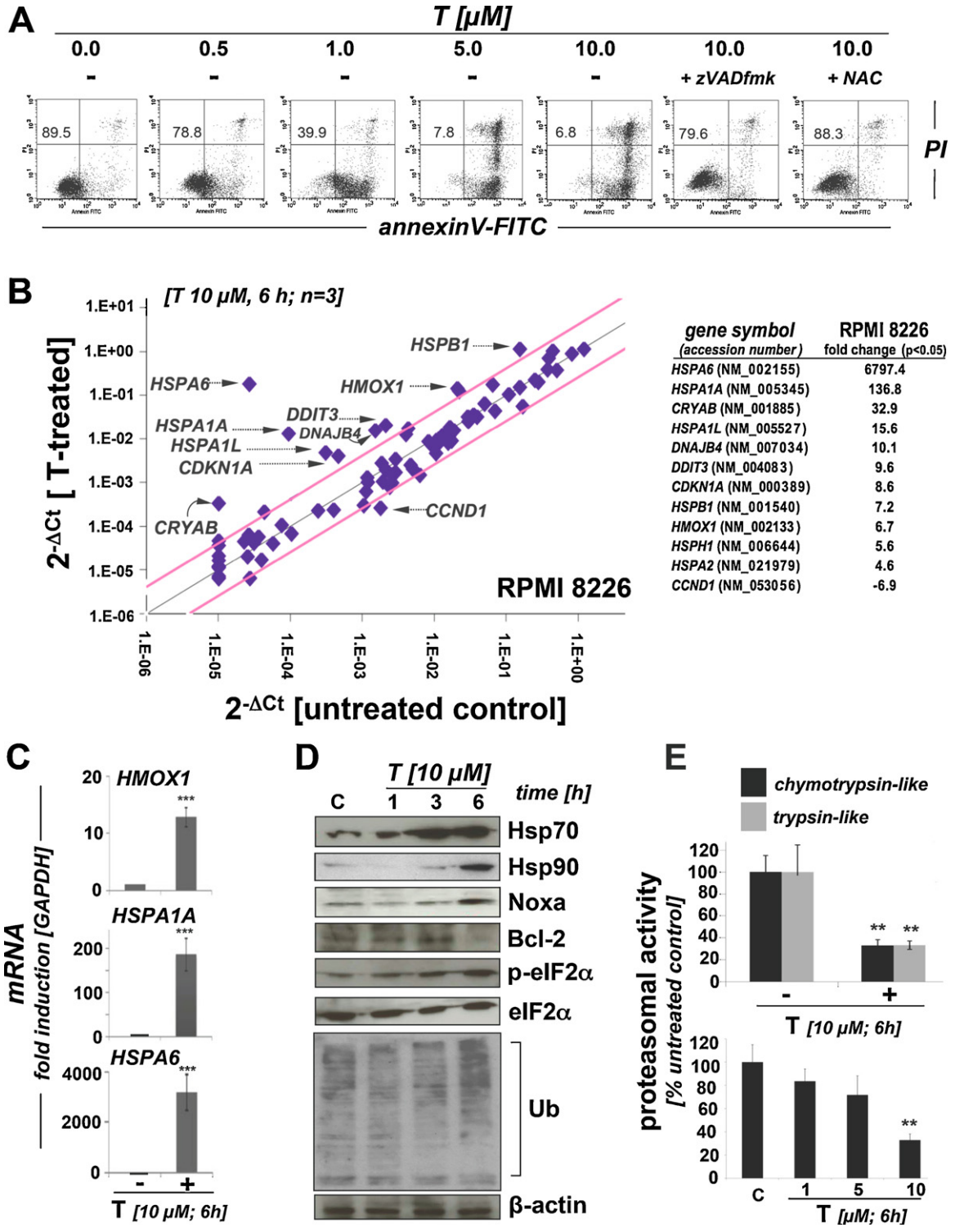

Fig. 5. Thiostrepton inhibits proteasome activity with induction of proteotoxic stress and apoptosis in human RPMI 8226 multiple myeloma cells. (A) Induction of cell death by exposure to T (0.5–10 μM, 24 h) in the absence or presence of zVADfmk (40 μM) or NAC (10 mM) was assessed by flow cytometric analysis. The numbers indicate viable (AV-, PI-) in percent of total gated cells. A representative experiment taken from three similar repeats is shown. (B) Gene expression array analysis of T-treated (10 μM, 6 h) RPMI 8226 cells. The scatter blot (left panel) depicts differential gene expression as detected by the RT^2 Human Stress and Toxicity Profiler^{TM} PCR Expression Array technology. Upper and lower lines: cut-off indicating fourfold up- or down-regulated expression, respectively. Arrays were performed in three independent repeats and analyzed using the two-sided Student's *t* test. The table (right panel) summarizes expression changes by at least four-fold ($p < 0.05$). (C) T-modulation (10 μM, 6 h) of *HMOX1*, *HSPA1A*, and *HSPA6* mRNA levels as assessed by independent real time RT-PCR analysis (mean ± SD, $n = 3$). (D) Immunoblot analysis examining T-modulation of proteotoxic stress markers and ubiquitination (10 μM, up to 6 h). (E) Inhibition of proteasomal enzymatic activity [up to 10 μM T, 6 h; upper panel: chymotrypsin-like versus trypsin-like activity; lower panel: chymotrypsin-like activity, dose–response relationship; mean ± SD; $n = 3$; * denotes statistically significant differences ($^*p < 0.05$; $^{**}p < 0.01$; $^{***}p < 0.001$)].

thiostrepton rapidly induces oxidative stress before proteasomal impairment becomes detectable and that thiostrepton-induced cell death and proteasome inhibition can both be antagonized by small molecule intervention using NAC.

3.5. Multiple myeloma cell-directed cytotoxicity of thiostrepton

Earlier work has demonstrated that multiple myeloma cells display a specific sensitivity to pharmacological proteasome inhibition, and the proteasome inhibitor bortezomib is now the FDA-approved standard of care for this malignancy [42,43]. We therefore tested feasibility of thiostrepton-based antimyeloma intervention examining cytotoxic effects in cultured human RPMI 8226 multiple myeloma cells (Fig. 5) [39,44]. Thiostrepton-induced apoptosis (24 h exposure time; Fig. 5A) occurred at submicromolar concentrations ($LD_{50} = 0.7 \pm 0.1$ μM; mean ± SD, $n = 3$), a dose that did not induce cell death in A375 melanoma cells (Fig. 1B). As observed with A375 cells (Fig. 1E), RPMI 8226 cell viability remained unimpaired at 6 h exposure time as assessed by trypan blue exclusion and annexinV-PI flow cytometry (data not shown), and zVADfmk pretreatment blocked thiostrepton-induced cell death consistent with a caspase-dependent mode of cell death (Fig. 5A). Moreover, antioxidant pretreatment (NAC; 10 mM) antagonized thiostrepton cytotoxicity in RPMI 8226 cells (Fig. 5A), and induction of cellular oxidative stress was apparent from increased DCF-fluorescence intensity that was upregulated within 1 h of continuous exposure (approximately nine-fold over untreated control cells; data not shown).

Next, early modulation of stress and toxicity response gene expression was examined in RPMI 8226 cells exposed to thiostrepton using the PCR Expression Array methodology as described above (Fig. 5B; 10 μM, 6 h exposure). As detected in A375 melanoma cells (Fig. 2A–C), massive upregulation of heat shock response gene expression was observed including genes encoding the heat shock proteins *Hsp70B′* (*HSPA6*; 6797-fold), *Hsp70 protein 1A* (*HSPA1A*; 137-fold), *alpha-crystallin B chain* (*CRYAB*; 33-fold), *Hsp70 protein 1-like* (*HSPA1L*; 16-fold), the Hsp70 cochaperone *DnaJ (Hsp40) homolog, subfamily B, member 4* (*DNAJB4*; 10 fold), *Hsp27 protein 1* (*HSPB1*; 7 fold), and *Hsp105 protein 1* (HSPH1, 6-fold). Moreover, upregulation of genes encoding the ER-stress responsive transcription factor *DNA damage* inducible transcript 3/CHOP (DDIT3/GADD153; 10-fold), the heat shock protein and antioxidant enzyme heme oxygenase-1 (HMOX1; 7-fold), and the p53-regulated inhibitor of cell cycle progression cyclin-dependent kinase inhibitor 1 (CDKN1A, 9-fold) was detected [31,45–47]. Strikingly, as observed earlier in A375 cells but not in primary melanocytes (Fig. 2A–C), thiostrepton significantly downregulated expression of *CCND1* (almost 7-fold), the gene encoding cyclin D1, an important proliferative factor driving cell cycle progression, known to be overexpressed in multiple myeloma [48].

Independent analysis by quantitative RT-PCR confirmed massive upregulation of *HSPA6* (over 3000-fold), *HSPA1A* (almost 200 fold), *and HMOX1 (over 10-fold)* expression at the mRNA level (Fig. 5C). At the protein level, immunoblot detection revealed rapid induction of proteotoxic stress and heat shock response as indicated by upregulation of Hsp70 and Hsp90 as well as phosphorylation of eIF2α, detectable within 3–6 h exposure time (Fig. 5D). Thiostrepton treatment caused proapoptotic modulation of Bcl-2 family members with upregulation of Noxa and down-regulation of Bcl-2 (Fig. 5D), whereas Bax levels remained unchanged (data not shown). Importantly, early thiostrepton-induced accumulation of ubiquitinated proteins was detected in total cellular extracts, a finding consistent with inhibition of proteasomal activity. Indeed, pronounced inhibition of chymotrypsin-like and trypsin-like proteolytic activity (by more than 70%) was detected, reaching the level of statistical significance at 10 μM thiostrepton (6 h exposure time) (Fig. 5 E).

4. Discussion

Pharmacological induction of proteotoxic stress has recently emerged as a promising strategy for chemotherapeutic intervention targeting cancer cells [36,42,49,50]. Proteotoxic stress occurs in response to cytotoxic stimuli that cause accumulation of unfolded and/or misfolded proteins including heat shock, oxidative stress, calcium dysregulation, and proteasome inhibition [38,43]. It is now widely accepted that tumor cells are exposed to high levels of endogenous proteotoxic stress originating from mutation-driven expression of misfolded proteins and adverse conditions associated with the tumor microenvironment including hypoxia, energy crisis, and redox dysregulation [51,52]. It has therefore been suggested that pharmacological induction of cytotoxic overload with dysfunctional proteins, either by causation of ROS-dependent protein unfolding or interference with proteolytic clearance, may trigger preferential apoptosis in cancer cells without compromising viability of normal cells displaying lower constitutive levels of endogenous oxidative and proteotoxic stress [15,36,42,49–51].

Here we demonstrate for the first time that thiostrepton displays dual activity as a prooxidant and proteotoxic chemotherapeutic targeting melanoma cells while sparing primary melanocytes (Figs. 1–4). As a likely mechanism of proteotoxic stress induction, we observed that at micromolar concentrations thiostrepton treatment was associated with inhibition of chymotrypsin-like but not trypsin-like proteasomal activity, an effect detected equally within 3 h exposure in human A375 metastatic melanoma cells and primary melanocytes (Fig. 3B and D). However, pronounced accumulation of ubiquitinated proteins above constitutive levels occurred only in melanoma cells treated with thiostrepton (Fig. 3A and C), indicating that partial proteasome inhibition by thiostrepton disrupts clearance of ubiquitinated proteins in melanoma cells but not in melanocytes.

Proteasome inhibitors including the boronic acid-tripeptide bortezomib are now FDA-approved for treating relapsed multiple myeloma, and other proteasome inhibitors including carfilzomib are in advanced stages of clinical development [53]. Therefore, we also evaluated the potential antimyeloma activity of thiostrepton focusing on human RPMI 8226 multiple myeloma cells, a cell line representative of the disease and displaying high sensitivity to pharmacological proteasome inhibition (Fig. 5) [39,44]. Indeed, rapid induction of proteotoxic and apoptogenic effects associated with proteasome inactivation and upregulated protein ubiquitination were observed in thiostrepton-treated RPMI 8226 cells (Fig. 5), and, in analogy to the effects observed earlier in A375 cells, massive induction of heat shock response gene expression was observed at the mRNA and protein level (Hsp70 and Hsp90) long before cell viability was impaired.

It is important to note that thiostrepton has been recognized before as a moderately potent inhibitor of proteasome activity [24,26], and synergistic cytotoxic effects were observed in cancer cell lines exposed to the combined action of bortezomib and thiostrepton [29]. Data obtained using the isolated human erythrocyte 20S proteasome suggest a mechanism of inhibition consistent with ligand-based partial antagonism and allosteric modulation [54]. In a recent study, structure–activity relationship of thiostrepton-induced proteasome inhibition was examined using various thiazole antibiotic analogues and derivatives of thiostrepton, among which only thiostrepton and siomycin A displayed considerable activity [26]. However, no thiostrepton-pharmacophore that would interact with a defined proteasomal target site was identified.

Our data obtained in A375 metastatic melanoma cells demonstrate that antioxidant treatment can antagonize thiostrepton-induced proteasomal inactivation (Fig. 4D). Interestingly, inactivation of proteasomal proteolytic activity by reactive oxygen species has been observed earlier [55,56], and based on the early occurrence of thiostrepton-induced oxidative stress that clearly precedes proteasome inhibition (Fig. 4A–B) it is therefore tempting to speculate that thiostrepton-induced oxidative stress is an upstream event that may contribute to proteasome inactivation. Thiostrepton-induced oxidative stress was detectable at very early time points as obvious from elevated DCF fluorescence intensity (1 h exposure time; Fig. 4A) and downregulation of cellular reduced glutathione (3 h; Fig. 4B). Pronounced upregulation of the antioxidant enzyme *HMOX1* was observed at the mRNA and protein level (6 h exposure; Fig. 2A and F). Treatment using the thiol-based antioxidant and disulfide-reducing agent NAC rescued cells from thiostrepton-induced loss of viability, whereas pharmacological glutathione depletion enhanced cytotoxicity (Fig. 4C), suggesting the causative involvement of oxidative stress in thiostrepton-induced cell death.

Early induction of oxidative stress that precedes proteasome inhibition is a specific feature of thiostrepton-induced cytotoxicity not shared by other proteasome inhibitors such as MG132 and bortezomib known to produce oxidative stress downstream of proteasomal and mitochondrial impairment [57,58]. However, the specific molecular mechanism underlying thiostrepton-induced dysregulation of cellular redox homeostasis observed by us is in cultured melanoma and myeloma cells remains to be elucidated, and numerous factors may contribute to thiostrepton-associated oxidative stress. For example, it has been shown earlier that spontaneous adduction of cellular thiol-residues by the electrophilic dehydroalanine-moieties of thiostrepton imparts antimicrobial activity through covalent modulation of microbial targets [22], and it is therefore possible that oxidative stress and glutathione depletion observed in melanoma cells result in part from covalent adduction of critical cellular thiol-residues, a hypothesis to be substantiated by future experimentation. An earlier report examining sensitization of cultured melanoma cells to arsenic trioxide-associated cytotoxicity has demonstrated thiostrepton-induced upregulation of oxidative stress together with mitochondrial dysfunction observed after 18 h continuous exposure [21], and prior research indicates that bortezomib-based proteasome inhibition can disrupt mitochondrial membrane integrity causing subsequent ROS formation and cellular oxidative stress [57]. However, our experiments indicate that thiostrepton-induced ROS formation occurs before impairment of proteasomal activity and without changes in melanoma cell mitochondrial transmembrane potential (as assessed by flow cytometric analysis of JC1-stained cells monitored over 12 h; data not shown), disqualifying the causative involvement of early proteasome inhibition or mitochondriotoxic effects in thiostrepton-induced early oxidative stress.

The specific molecular role of oxidative and proteotoxic stress in thiostrepton-induced melanoma and myeloma cell apoptosis remains unexplored at this point and may include modulation of various key targets. It has been shown earlier that proteasome inhibitors (including MG-132, lactacystin, and bortezomib) trigger Noxa-mediated apoptosis in metastatic melanoma and myeloma cells [39,40], and thiostrepton-dependent Noxa upregulation has indeed been observed in HCT116 colon and MCF7 breast carcinoma cells after 24 h continuous exposure [59]. Earlier research indicates that modulation of Noxa protein levels that would facilitate Bax-dependent mitochondrial apoptosis may occur as a result of various upstream events including p53-dependent transcriptional activation of *PMAIP1*, the gene encoding Noxa, and p53-independent inhibition of proteasomal degradation of Noxa [39,41,60]. Consequently, thiostrepton-induced proteasome inhibition may cause accumulation of apoptotic regulators known to be controlled by proteasomal degradation including Noxa, Mcl-1, and p53 as observed in our experiments (Fig. 2F), a finding consistent with earlier research that has documented accumulation of Mcl-1 and Noxa in bortezomib-treated melanoma and chronic lymphocytic leukemia (CLL) cells [39–41]. In addition, Bcl-2-downregulation, observed by us in thiostrepton-treated melanoma (Fig. 2F) and myeloma cells (Fig. 5D) but not melanocytes (Fig. 2H), has been shown earlier to result from elevated expression of the ER stress-responsive transcription factor CHOP encoded by *DDIT3* (*Gadd153*), a gene significantly upregulated in our experiments as detected by expression array analysis (Figs. 2A and 5B) [61].

Earlier research has identified the negative regulation of the oncogenic transcription factor FoxM1 by proteasome inhibitors, thought to represent an important molecular factor involved in cancer cell-directed cytotoxicity of thiostrepton [28,62,63]. However, previous work documenting thiostrepton-modulation of *FOXM1* expression in metastatic melanoma cells has only examined effects of prolonged exposure ($\geq$ 24 h exposure time) [30]. Our own data on A375 melanoma cells do not indicate early expression changes (within 12 h exposure) at the mRNA or protein level (data not shown). Future experiments must therefore aim at dissecting the mechanistic relationship between thiostrepton-induced early cellular changes observed in our experiments (redox dysregulation, proteotoxic stress, and mitochondrial apoptosis) and modulation of other potentially crucial targets including FoxM1 examined by others in much detail [27,64].

Taken together, our findings demonstrate that thiostrepton displays dual activity as a selective prooxidant and proteotoxic chemotherapeutic targeting human metastatic melanoma cells without compromising viability of primary melanocytes. Remarkably, thiostrepton is an FDA-approved antimicrobial drug used in combination with nystatin and neomycin in veterinary applications [65]. Combined with recent evidence demonstrating efficacy and tolerability of systemic administration of thiostrepton polyethylene glycol-encapsulated nanoformulations in various murine xenograft models [25], further preclinical experimentation should aim at testing feasibility of thiostrepton-based experimental chemotherapy targeting metastatic melanoma and other malignancies including multiple myeloma.

Acknowledgements

Supported in part by grants from the National Institutes of Health [R01CA122484, ES007091, ES06694, Arizona Cancer Center Support Grant CA023074]. The content is solely the responsibility of the authors and does not necessarily represent the official views of the National Cancer Institute or the National Institutes of Health.

References

[1] Garbe C, Eigentler TK, Keilholz U, Hauschild A, Kirkwood JM. Systematic review of medical treatment in melanoma: current status and future prospects. Oncologist 2011;16:5–24.
[2] Aplin AE, Kaplan FM, Shao Y. Mechanisms of resistance to RAF inhibitors in melanoma. J Invest Dermatol 2011;131:1817–20.
[3] Meyskens Jr FL, Buckmeier JA, McNulty SE, Tohidian NB. Activation of nuclear factor-kappa B in human metastatic melanoma cells and the effect of oxidative stress. Clin Cancer Res 1999;5:1197–202.
[4] Govindarajan B, Sligh JE, Vincent BJ, Li M, Canter JA, Nickoloff BJ, et al. Overexpression of Akt converts radial growth melanoma to vertical growth melanoma. J Clin Invest 2007;117:719–29.
[5] Fried L, Arbiser JL. The reactive oxygen-driven tumor: relevance to melanoma. Pigment Cell Melanoma Res 2008;21:117–22.
[6] Fruehauf JP, Trapp V. Reactive oxygen species: an Achilles' heel of melanoma. Expert Rev Anticancer Ther 2008;8:1751–7.
[7] Laurent A, Nicco C, Chereau C, Goulvestre C, Alexandre J, Alves A, et al. Controlling tumor growth by modulating endogenous production of reactive oxygen species. Cancer Res 2005;65:948–56.

[8] Cabello CM, Bair 3rd WB, Wondrak GT. Experimental therapeutics: targeting the redox Achilles heel of cancer. Curr Opin Investig Drugs 2007;8:1022–37.
[9] Trachootham D, Alexandre J, Huang P. Targeting cancer cells by ROS-mediated mechanisms: a radical therapeutic approach. Nat Rev Drug Discov 2009; 8:579–91.
[10] Raj L, Ide T, Gurkar AU, Foley M, Schenone M, Li X, et al. Selective killing of cancer cells by a small molecule targeting the stress response to ROS. Nature 2011;475:231–4.
[11] Trachootham D, Zhou Y, Zhang H, Demizu Y, Chen Z, Pelicano H, et al. Selective killing of oncogenically transformed cells through a ROS-mediated mechanism by beta-phenylethyl isothiocyanate. Cancer Cell 2006;10:241–52.
[12] Alexandre J, Nicco C, Chereau C, Laurent A, Weill B, Goldwasser F, et al. Improvement of the therapeutic index of anticancer drugs by the superoxide dismutase mimic mangafodipir. J Natl Cancer Inst 2006;98:236–44.
[13] Cabello CM, Bair 3rd WB, Bause AS, Wondrak GT. Antimelanoma activity of the redox dye DCPIP (2,6-dichlorophenolindophenol) is antagonized by NQO1. Biochem Pharmacol 2009;78:344–54.
[14] Townsend DM, He L, Hutchens S, Garrett TE, Pazoles CJ, Tew KD. NOV-002, a glutathione disulfide mimetic, as a modulator of cellular redox balance. Cancer Res 2008;68:2870–7.
[15] Hancock CN, Stockwin LH, Han B, Divelbiss RD, Jun JH, Malhotra SV, et al. A copper chelate of thiosemicarbazone NSC 689534 induces oxidative/ER stress and inhibits tumor growth in vitro and in vivo. Free Radic Biol Med 2011;50:110–21.
[16] Ramanathan RK, Abbruzzese J, Dragovich T, Kirkpatrick L, Guillen JM, Baker AF, et al. A randomized phase II study of PX-12, an inhibitor of thioredoxin in patients with advanced cancer of the pancreas following progression after a gemcitabine-containing combination. Cancer Chemother Pharmacol 2011; 67:503–9.
[17] Wondrak GT. Redox-directed cancer therapeutics: molecular mechanisms and opportunities. Antioxid Redox Signal 2009;11:3013–69.
[18] Tew KD, Townsend DM. Redox platforms in cancer drug discovery and development. Curr Opin Chem Biol 2011;15:156–61.
[19] Montero AJ, Jassem J. Cellular redox pathways as a therapeutic target in the treatment of cancer. Drugs 2011;71:1385–96.
[20] Cabello CM, Lamore SD, Bair 3rd WB, Qiao S, Lesson JL, Wondrak GT. The redox antimalarial dihydroartemisinin targets human metastatic melanoma cells but not primary melanocytes with induction of NOXA-dependent apoptosis. Invest New Drugs 2011 [Epub ahead of print].
[21] Bowling BD, Doudican N, Manga P, Orlow SJ. Inhibition of mitochondrial protein translation sensitizes melanoma cells to arsenic trioxide cytotoxicity via a reactive oxygen species dependent mechanism. Cancer Chemother Pharmacol 2008;63:37–43.
[22] Chiu ML, Folcher M, Griffin P, Holt T, Klatt T, Thompson CJ. Characterization of the covalent binding of thiostrepton to a thiostrepton-induced protein from Streptomyces lividans. Biochemistry 1996;35:2332–41.
[23] Harms JM, Wilson DN, Schluenzen F, Connell SR, Stachelhaus T, Zaborowska Z, et al. Translational regulation via L11: molecular switches on the ribosome turned on and off by thiostrepton and micrococcin. Mol Cell 2008;30:26–38.
[24] Aminake MN, Schoof S, Sologub L, Leubner M, Kirschner M, Arndt HD, et al. Thiostrepton and derivatives exhibit antimalarial and gametocytocidal activity by dually targeting parasite proteasome and apicoplast. Antimicrob Agents Chemother 2011;55:1338–48.
[25] Wang M, Gartel AL. Micelle-encapsulated thiostrepton as an effective nanomedicine for inhibiting tumor growth and for suppressing FOXM1 in human xenografts. Mol Cancer Ther 2011 [Epub ahead of print].
[26] Pandit B, Bhat UG, Gartel AL. Proteasome inhibitory activity of thiazole antibiotics. Cancer Biol Ther 2011;11:43–7.
[27] Kwok JM, Myatt SS, Marson CM, Coombes RC, Constantinidou D, Lam EW. Thiostrepton selectively targets breast cancer cells through inhibition of forkhead box M1 expression. Mol Cancer Ther 2008;7:2022–32.
[28] Bhat UG, Halasi M, Gartel AL. FoxM1 is a general target for proteasome inhibitors. PLoS One 2009;4:e6593.
[29] Pandit B, Gartel AL. Thiazole antibiotic thiostrepton synergize with bortezomib to induce apoptosis in cancer cells. PLoS One 2011;6:e17110.
[30] Bhat UG, Zipfel PA, Tyler DS, Gartel AL. Novel anticancer compounds induce apoptosis in melanoma cells. Cell Cycle 2008;7:1851–5.
[31] Cabello CM, Bair 3rd WB, Ley S, Lamore SD, Azimian S, Wondrak GT. The experimental chemotherapeutic N(6)-furfuryladenosine (kinetin-riboside) induces rapid ATP depletion, genotoxic stress, and CDKN1A (p21) upregulation in human cancer cell lines. Biochem Pharmacol 2009;77:1125–38.
[32] Cabello CM, Bair 3rd WB, Lamore SD, Bause AS, Azimian S, Wondrak GT. The cinnamon-derived Michael acceptor cinnamic aldehyde impairs melanoma cell proliferation, invasiveness, and tumor growth. Free Radic Biol Med 2009;46:220–31.
[33] Lamore SD, Cabello CM, Wondrak GT. The topical antimicrobial zinc pyrithione is a heat shock response inducer that causes DNA damage and PARP-dependent energy crisis in human skin cells. Cell Stress Chaperones 2010;15:309–22.
[34] Wondrak GT. NQO1-activated phenothiazinium redox cyclers for the targeted bioreductive induction of cancer cell apoptosis. Free Radic Biol Med 2007;43:178–90.
[35] Cabello CM, Lamore SD, Bair WB, Davis AL, Azimian SM, Wondrak GT. DCPIP (2,6-dichlorophenolindophenol) as a genotype-directed redox chemotherapeutic targeting NQO1*2 breast carcinoma. Free Radic Res 2011;45:276–92.
[36] Healy SJ, Gorman AM, Mousavi-Shafaei P, Gupta S, Samali A. Targeting the endoplasmic reticulum-stress response as an anticancer strategy. Eur J Pharmacol 2009;625:234–46.
[37] Noonan EJ, Place RF, Giardina C, Hightower LE. Hsp70B' regulation and function. Cell Stress Chaperones 2007;12:219–29.
[38] Kim I, Xu W, Reed JC. Cell death and endoplasmic reticulum stress: disease relevance and therapeutic opportunities. Nat Rev Drug Discov 2008;7:1013–30.
[39] Qin JZ, Ziffra J, Stennett L, Bodner B, Bonish BK, Chaturvedi V, et al. Proteasome inhibitors trigger NOXA-mediated apoptosis in melanoma and myeloma cells. Cancer Res 2005;65:6282–93.
[40] Fernandez Y, Verhaegen M, Miller TP, Rush JL, Steiner P, Opipari Jr AW, et al. Differential regulation of Noxa in normal melanocytes and melanoma cells by proteasome inhibition: Therapeutic implications. Cancer Res 2005;65:6294–304.
[41] Baou M, Kohlhaas SL, Butterworth M, Vogler M, Dinsdale D, Walewska R, et al. Role of NOXA and its ubiquitination in proteasome inhibitor-induced apoptosis in chronic lymphocytic leukemia cells. Haematologica 2010;95:1510–8.
[42] Obeng EA, Carlson LM, Gutman DM, Harrington Jr WJ, Lee KP, Boise LH. Proteasome inhibitors induce a terminal unfolded protein response in multiple myeloma cells. Blood 2006;107:4907–16.
[43] Chen D, Frezza M, Schmitt S, Kanwar J, Dou QP. Bortezomib as the first proteasome inhibitor anticancer drug: current status and future perspectives. Curr Cancer Drug Targets 2011;11:239–53.
[44] Matsuoka Y, Moore GE, Yagi Y, Pressman D. Production of free light chains of immunoglobulin by a hematopoietic cell line derived from a patient with multiple myeloma. Proc Soc Exp Biol Med 1967;125:1246–50.
[45] Sarkar D, Su ZZ, Lebedeva IV, Sauane M, Gopalkrishnan RV, Valerie K, et al. Mda-7 (IL-24) mediates selective apoptosis in human melanoma cells by inducing the coordinated overexpression of the GADD family of genes by means of p38 MAPK. Proc Natl Acad Sci U S A 2002;99:10054–59.
[46] Scott DW, Loo G. Curcumin-induced GADD153 gene up-regulation in human colon cancer cells. Carcinogenesis 2004;25:2155–64.
[47] O'Reilly MA. Redox activation of p21Cip1/WAF1/Sdi1: a multifunctional regulator of cell survival and death. Antioxid Redox Signal 2005;7:108–18.
[48] Bergsagel PL, Kuehl WM, Zhan F, Sawyer J, Barlogie B, Shaughnessy Jr J. Cyclin D dysregulation: an early and unifying pathogenic event in multiple myeloma. Blood 2005;106:296–303.
[49] De Raedt T, Walton Z, Yecies JL, Li D, Chen Y, Malone CF, et al. Exploiting cancer cell vulnerabilities to develop a combination therapy for ras-driven tumors. Cancer Cell 2011;20:400–13.
[50] Xu W, Trepel J, Ras NL. ROS and proteotoxic stress: a delicate balance. Cancer Cell 2011;20:281–2.
[51] Luo J, Solimini NL, Elledge SJ. Principles of cancer therapy: oncogene and non-oncogene addiction. Cell 2009;136:823–37.
[52] Dai C, Dai S, Cao J. Proteotoxic stress of cancer: implication of the heat-shock response in oncogenesis. J Cell Physiol 2011.
[53] Dasmahapatra G, Lembersky D, Son MP, Attkisson E, Dent P, Fisher RI, et al. Carfilzomib interacts synergistically with histone deacetylase inhibitors in mantle cell lymphoma cells in vitro and in vivo. Mol Cancer Ther 2011;10:1686–97.
[54] Schoof S, Pradel G, Aminake MN, Ellinger B, Baumann S, Potowski M, et al. Antiplasmodial thiostrepton derivatives: proteasome inhibitors with a dual mode of action. Angew Chem Int Ed Engl 2010;49:3317–21.
[55] Reinheckel T, Sitte N, Ullrich O, Kuckelkorn U, Davies KJ, Grune T. Comparative resistance of the 20S and 26S proteasome to oxidative stress. Biochem J 1998;335(Pt 3):637–42.
[56] Breusing N, Grune T. Regulation of proteasome-mediated protein degradation during oxidative stress and aging. Biol Chem 2008;389:203–9.
[57] Ling YH, Liebes L, Zou Y, Perez-Soler R. Reactive oxygen species generation and mitochondrial dysfunction in the apoptotic response to Bortezomib, a novel proteasome inhibitor, in human H460 non-small cell lung cancer cells. J Biol Chem 2003;278:33714–23.
[58] Fan WH, Hou Y, Meng FK, Wang XF, Luo YN, Ge PF. Proteasome inhibitor MG-132 induces C6 glioma cell apoptosis via oxidative stress. Acta Pharmacol Sin 2011;32:619–25.
[59] Pandit B, Gartel AL. Proteasome inhibitors induce p53-independent apoptosis in human cancer cells. Am J Pathol 2011;178:355–60.
[60] Ploner C, Kofler R, Villunger A. Noxa: at the tip of the balance between life and death. Oncogene 2008;27(Suppl. 1):S84–92.
[61] McCullough KD, Martindale JL, Klotz LO, Aw TY, Holbrook NJ. Gadd153 sensitizes cells to endoplasmic reticulum stress by down-regulating Bcl2 and perturbing the cellular redox state. Mol Cell Biol 2001;21:1249–59.
[62] Bhat UG, Halasi M, Gartel AL. Thiazole antibiotics target FoxM1 and induce apoptosis in human cancer cells. PLoS One 2009;4:e5592.
[63] Pandit B, Gartel AL. FoxM1 knockdown sensitizes human cancer cells to proteasome inhibitor-induced apoptosis but not to autophagy. Cell Cycle 2011;10:3269–73.
[64] Radhakrishnan SK, Bhat UG, Hughes DE, Wang IC, Costa RH, Gartel AL. Identification of a chemical inhibitor of the oncogenic transcription factor forkhead box M1. Cancer Res 2006;66:9731–5.
[65] Nesbitt GH, Fox PR. Clinical evaluation of Panolog Cream used to treat canine and feline dermatoses. Vet Med Small Anim Clin 1981;76:535–8.